

1 *Type of the Paper (Article)*

2 **Meander microwave bandpass filter on flexible** 3 **textile substrate**

4
5 Bahareh Moradi *, Raul Fernández-García and Ignacio Gil
6 Universitat Politècnica de Catalunya, Terrassa 08222, Barcelona, Spain

7 *Correspondence: bahareh.moradi@upc.edu

8

9 **Abstract:** This paper presents an alternative process to fabricate flexible bandpass filters by using
10 embroidered yarn conductor on electronic-textile. The novelty of the proposed miniaturized filter
11 is its complete integration on the outfit, with benefits in terms of compressibility, stretch ability and
12 high geometrical accuracy, opening the way to develop textile filters in sport and medicine wearable
13 applications. The proposed design consists of a fully embroidered microstrip topology with a length
14 equal to quarter wavelength ($\lambda/4$) to develop a bandpass filter frequency response. A drastic
15 reduction in size of the filter was achieved by taking advantage of a simplified architecture based
16 on meandered-line stepped impedance resonator. The e-textile microstrip filter has been designed,
17 simulated, fabricated and measured, with experimental validation at a 7.58 GHz frequency. The
18 insertion loss obtained by simulation of the filter is substantially small. The return loss is greater
19 than 20 dB for bands. To explore the relations between physical parameters and filter performance
20 characteristics, theoretical equivalent circuit model of the filter constituent components were
21 studied. The effect of bending of the e-textile filter is also studied. The results show that by changing
22 the radius of bending up to 40 mm, the resonance frequency is shifted up 4.25 MHz/mm.

23

24 **Keywords:** Band-pass filter, E-textile, Stepped impedance resonator, Meandered resonator

25

26 **1. Introduction**

27 Microwave band pass filters (BPF) are key building elements of communication systems. They
28 should satisfy severe requirements, mainly system performance frequency response, reduced size,
29 and manufacturing cost. Nowadays, several researches in the microwave domain are focused on BPF
30 size miniaturization and integration.

31 Recently, it is desirable to develop new type of microstrip band pass filters with small size and
32 planar fabrication. Parallel coupled microstrip band pass filters are common elements in many
33 microwave systems [1], due to their advantages such as planar design, easy analysis and low cost. A
34 type of miniaturized microstrip band pass filter by using pseudo-interdigital structure without via
35 holes ground is proposed in [1] and a variety of resonator types have been introduced including split-
36 ring resonators [2] or stepped impedance resonators (SIR) [3] to achieve band pass filter frequency
37 responses.

38 On the other hand, wearable technology has been widely developed and deeply studied in
39 recent years. It has been adopted in many applications including on-body networks [4], location
40 tracking [5], fitness monitoring [6], and e-textile metamaterial signal propagation control [7]. The
41 common features of e-textile systems are low-profile, light-weight, wireless connection and multi
42 functionality, required by modern wearable applications.

43 In this paper, we present for the first time an e-textile microwave filter based on embroidered
44 meander microstrip line. The new microstrip filter structure has advantages in terms of
45 compressibility, stretchability, and high duration to repetitive deformations. Results demonstrate
46 that the new textile filter has comparable performance to their conventional counterparts
47 implemented on conventional printed circuit board (PCB) substrates.

48 The main novelty of the paper consists of utilizing textile material as substrate to develop a
49 meander filter at the microwave frequency band. In comparison with conventional devices, the
50 proposed filter has the ability of controllable electromagnetic properties and device flexibility.
51 Furthermore, the proposed filter guarantees a band pass from 7.17 to 8 GHz with return loss lower
52 than -30 dB.

53 The e-textile filter has been simulated, fabricated and measured in the bandwidth delimited by
54 7.17-8 GHz with center frequency at 7.58 GHz.

55 The remainder of the paper is organized as follows. Section 2 describes the theoretical
56 framework of the proposed wearable meander microwave filter. In Section 3 the filter
57 implementation and experimental results are shown and discussed. In Section 4, the bending effects
58 on the filter performance are analysed experimentally. Finally, in Section 5 the conclusions of this
59 work are summarized.

60

61 2. THEORETICAL FRAMEWORK

62 The proposed band pass filter (BPF) is designed on an e-textile felt substrate with characterized
63 $h = 1$ mm thickness, dielectric constant $\epsilon_r = 1.2$, and loss tangent $\tan \delta = 0.0013$. In order to determine
64 the substrate dielectric constant and loss tangent of felt substrate, the resonance method based on a
65 split post dielectric resonator (SPDR) measurement has been carried out.

66 The filter is designed using a quarter wavelength ($\lambda/4$) microstrip with different characteristics
67 impedance of the line to achieve stepped impedance.

68 Since most filters are composed of linear components based on simple and fast computer-aided
69 network analyses, let us consider at first the stepped impedance resonators (SIR) concept. SIR allows
70 to establish a relation between the linear elements equivalent circuit model and the layout of physical
71 dimensions.

72 A microstrip stepped impedance resonator is formed by joining two transmission line with
73 different characteristic impedances, Z_1 and Z_2 , with corresponding electrical length θ_1 and θ_2 ,
74 respectively [8], as shown in Figure 1. Resonant condition of the SIR depends on value of θ_1, θ_2 and
75 R . Furthermore, the analytical models are used to compute the circuit parameters at 7.58 GHz central
76 frequency. The total electrical length of the structural fundamental is given by [9] which is $\theta_t = \theta_1 +$
77 $\theta_2, K < 1$. The resonance condition of an SIR will occur when,

$$78 \quad K = \tan \theta_1 \tan \theta_2 = \frac{Z_1}{Z_2} \quad (1)$$

79 Where K is impedance ratio. For this design we have considered $K=0.4$. The characteristic impedance
80 of lines are designed at $Z_1 = 50 \Omega$, $Z_2 = 121 \Omega$ and electrical lengths of line are $\theta_1 = 31^\circ$, $\theta_2 = 79^\circ$.

81

82

83

84

85

86

87

88

89

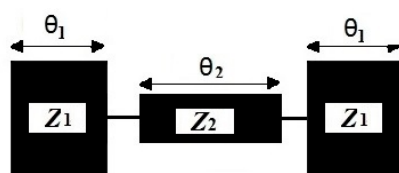


Figure 1. Configuration of the basic structure of the stepped impedance resonator (SIR), where $K = \frac{Z_1}{Z_2} < 1$.

The typical structure of the SIR as shown in Figure 1 can be mathematically verified by solving this electrical network using circuit theory. Over all ABCD parameters of this circuit are calculated by calculating ABCD parameters of the individual stepped. The ABCD parameters of the circuit can be determined by [10], as follows:

$$\begin{pmatrix} A & B \\ C & D \end{pmatrix}_{overall} = \begin{pmatrix} \cos \theta_1 & jZ_1 \sin \theta_1 \\ \frac{j \sin \theta_1}{Z_1} & \cos \theta_1 \end{pmatrix}_{step1} \begin{pmatrix} \cos \theta_2 & jZ_2 \sin \theta_2 \\ \frac{j \sin \theta_2}{Z_2} & \cos \theta_2 \end{pmatrix}_{step2} \begin{pmatrix} \cos \theta_1 & jZ_1 \sin \theta_1 \\ \frac{j \sin \theta_1}{Z_1} & \cos \theta_1 \end{pmatrix}_{step1} \quad (2)$$

Where, A, B, C, and D are the network parameters of the transmission matrix, which is the result of the multiplication of the three ABCD matrices corresponding to network of Figure 1.

In order to reduce the filter size, in next step the meandered line SIR was considered. The layout of the proposed filter is illustrated in Figure 2 (a) that, the line width for microstrip is chosen as $W_1 = 4$ mm, which gives characteristic impedance $Z_0 = 50$ ohm on the substrate. The detailed dimensions are as follows: $L_{S1} = 3.26$ mm, $L_{S2} = 18.5$ mm, $L_{S3} = 1.5$ mm, and spacing between two meander lines $S = 1.5$ mm. Also width for microstrip quarter -wavelength resonators is chosen as $W_2 = 0.5$ mm.

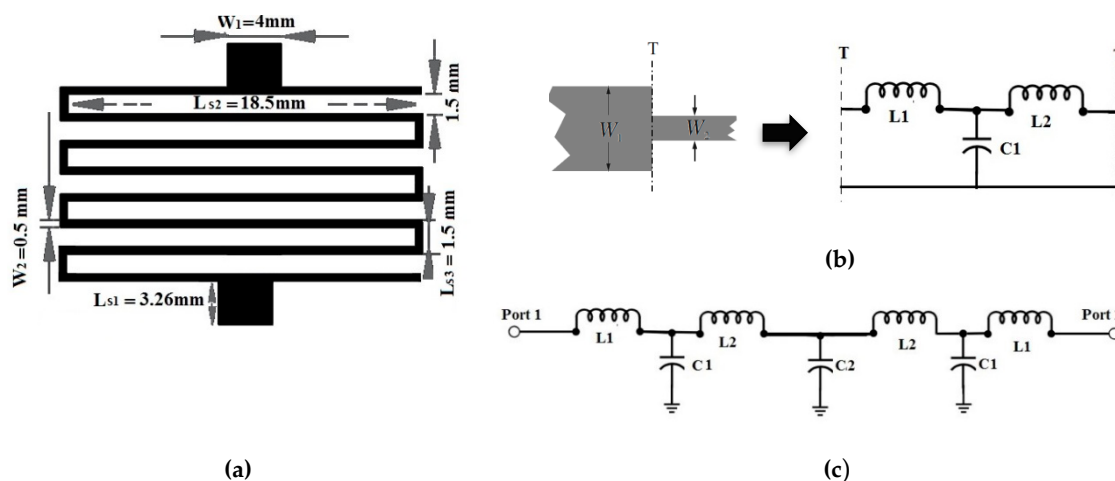


Figure 2. (a) Layout of the proposed e-textile meander microstrip line. (b) Capacitance and inductances of the equivalent circuits for the subnetworks for symmetrical steps. (c) Equivalent circuit model of network.

The equivalent circuit model of a filter helps to understand the behavior of the design. As illustrated in Figure 2(b), the subnetwork can be represented by L-C circuit and the values of L and C of individual steps is calculated by the use of standard equations in [8]. For the symmetrical microstrip steps the subnetworks is described by capacitance (C_1) and inductances (L_1, L_2) corresponding to equivalent circuit shown in Figure 2(b). In the other hand, the proposed meander microstrip lines

137 acts as a resonant (L_2C_2) circuit. The vertical elements act as the inductor, horizontal elements act as
 138 capacitor. The overall electrical equivalent circuit of the proposed filter structure which is shown in
 139 Figure 2(c) can be obtained by combining the equivalent circuits of symmetrical steps and meander
 140 microstrip lines. This circuit is simulated by Advanced Design System (ADS) simulator and its
 141 frequency response is compared with full 3D electromagnetic CST Microwave Studio 2018 software.
 142 The capacitance and inductances of the equivalent circuit indicated in Figure 2(c) can be
 143 approximated by the following formulation [8].

$$144 \quad C_1 = 0.00137h \frac{\sqrt{\epsilon_{re}}}{Z_{c1}} \left(1 - \frac{W_2}{W_1}\right) \left(\frac{\epsilon_{re1}+0.3}{\epsilon_{re1}-0.258}\right) \left(\frac{W_1/h+0.264}{W_1/h+0.8}\right) \quad (pF) \quad (3)$$

145 The estimation of the capacitance of the interdigital layout can be given by

$$146 \quad C_2 = 3.937 \times 10^{-5} l (\epsilon_r + 1)(0.11(N - 3) + 0.252) \quad (pF) \quad (4)$$

147 The total length is given by $\frac{\lambda_0}{4} = NL_2 + (N - 1)S$ where N number of turns, S is spacing between
 148 two meander lines. The inductance per unit length is calculated as follows [8]:

$$149 \quad L = 0.000987h \left(1 - \frac{Z_{c1}}{Z_{c2}} \sqrt{\frac{\epsilon_{re1}}{\epsilon_{re2}}}\right)^2 \quad (nH) \quad (5)$$

$$150 \quad L_{w1} = \frac{Z_{c1}\sqrt{\epsilon_{re1}}}{c} \quad \text{and} \quad L_{w2} = \frac{Z_{c2}\sqrt{\epsilon_{re2}}}{c} \quad (6)$$

151 Where L_{wi} for $i = 1, 2$ are the inductances per unit length, having widths W_1 and W_2 , respectively.
 152 While Z_{Ci} and ϵ_{rei} denote the characteristic impedance and effective dielectric constant
 153 corresponding to width W_i and c is the light velocity in free space.

$$154 \quad L_1 = \frac{L_{w1}}{L_{w1}+L_{w2}} L \quad (nH) \quad \text{and} \quad L_2 = \frac{L_{w2}}{L_{w1}+L_{w2}} L \quad (nH) \quad (7)$$

155 The values of the different parameters can be initially estimated from the physical dimensions, but at
 156 the end there will be necessary to optimize them by a tuning procedure to fit the measured response.

162 3. Filter Implementation and Results

163 The fabric structure was a non-woven structure with a 100% polyester composition. These textile
 164 substrates are resistant to sweat and humidity and they offer some key advantages, including
 165 durability, chemical moisture resistance, and heat stability. The weight is 211 g/m², and the structure
 166 is a double-sided needle punching.

167 The selected conductor yarn corresponds to a commercial Shieldex Plated Nylon 66 Yarn 117/17
 168 dtex 2- ply and it is composed by 99% pure silver plated nylon yarn 140/17 dtex with a linear
 169 resistance < 30 Ω /cm. The used stitch type corresponds to the ISO 4915:1991 301 standard.

170 The conductive thread is relatively thick compared to the conventional embroidery thread, due
 171 to the mechanical restrictions of the embroidery machine. In order to optimize the fabrication process
 172 the conductive thread has been used in the bobbin of the embroidery machine whereas a conventional
 173 embroidery yarn has been considered for the upper thread. A certain degree of tension control in the
 174 upper thread is carried out in order to increase the accuracy of the stitching geometries and patterns.
 175 The stitch spacing corresponds to the distance between two needle penetrations on the same side of
 176 a column. The homogeneous layout is converted to a stitch pattern by using the *Digitizer Ex* software
 177 for fabrication process. This software package is used to create the stitch pattern, which is then
 178 exported to the embroidery machine and stitched. A *Singer Futura XL-550* embroidery machine has
 179 been used to manufacture the prototype.

180 The proposed design has been embroidered with satin pattern with 60% density. The density
 181 determines the gap between stitches. For narrow columns, stitches are tight, thus requiring fewer
 182 stitches to cover the fabric. In areas with very narrow columns, less dense stitches are required
 183 because too many needle penetrations can damage the textile sample. Indeed by increasing
 184 embroidering density boost surface conductivity.

185 The ground plane had been chosen as a homogeneous uniform commercial *WE-CF* adhesive
 186 copper sheet layer (constant thickness $t = 35 \mu\text{m}$).

187 Figure 3 shows the photograph of the BPF embroidered wearable prototype. The idea is to use
 188 e-textile to enable low embroidery tension and high flexibility, improving the embroidery process.
 189 The fabricated filter satisfied the requirements of providing the wearer with such compact size,
 190 flexible materials, ease of washing, and very attractive wearable application.

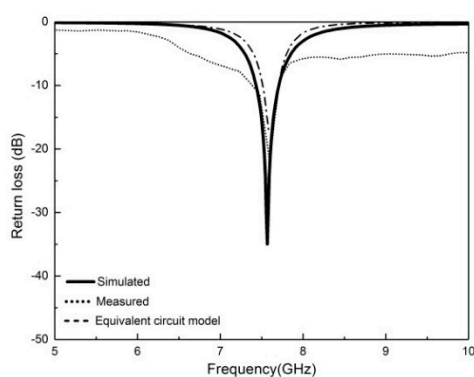


201
202 **Figure 3.** Photograph of the embroidered design.

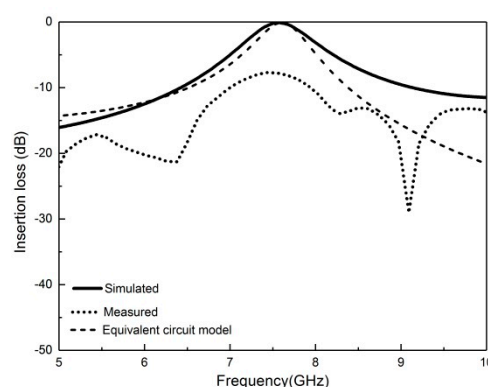
203
204 Figure 4 shows the comparison between the simulated and measured frequency responses of
 205 insertion losses (S_{21}) return losses (S_{11}). The S_{21} and S_{11} were tested up to 10 GHz by means of a
 206 microwave analyzer, *N9916A FieldFox* (Keysight, Santa Rosa, CA, USA), operating as a vector
 207 network analyzer.

208 As illustrated in Figures 4(a, b), the bandwidth of the simulated and equivalent circuit model
 209 results was in the range between 7.17 GHz and 8 GHz. Furthermore, there is a clear relationship
 210 between the equivalent circuit model and the layout physical dimensions.

211 The simulated and equivalent circuit model of proposed circuit presents good electrical
 212 performances with an insertion loss of -0.5 dB and a return loss of -30 dB at the frequency (7.58 GHz),
 213 whereas the measured insertion loss and the return loss are about -11dB and -29 dB respectively. The
 214 discrepancy between simulated and measured results is due to fabrication tolerances, thickness of
 215 the adhesive that was used for ground layer, and improper soldering of connector as well as the lack
 216 of homogeneity of the embroidery, in comparison with standard PCB metallization. Nevertheless,
 217 the bandpass behavior is clearly defined and can be boosted by a conventional amplification
 218 technique.



220
221
222
223
224
225
226
227
228
229
230
231
232 (a)



(b)

233 **Figure 4.** Comparison between insertion loss and the return loss measured, electromagnetically simulated
 234 and equivalent circuit response of band pass filter.
 235

236 The equivalent circuit parameters are extracted from optimization of circuit to fit with the
 237 simulated and measured response. Table I shows a summary of parameters corresponding to
 238 capacitance and inductances parameters of Figure 2(c), for the best fit we have been able to find in
 239 simulation and theoretical point of view.
 240

241 Table I: Comparison of equivalent circuit model parameters in simulation (ADS) and theoretical of band pass filter

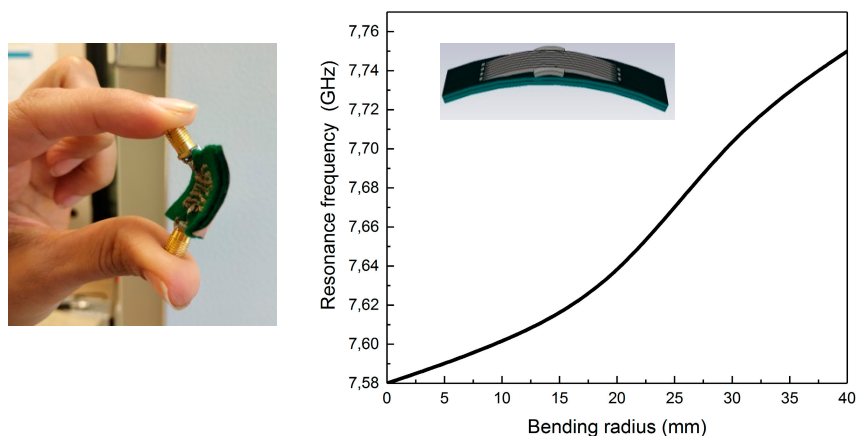
Comparison	L_1 (nH)	L_2 (nH)	C_1 (pF)	C_2 (pF)
Theoretical parameters	0.96	2.32	$1.7e^{-6}$	1.1
Optimized Parameters	0.03	6.4	$0.05e^{-6}$	0.13

242
 243

244 4. Bending Effects

245 In wearable systems, it is very difficult to keep the substrate in a flat configuration all the time,
 246 especially when the prototype is made of textile materials and it is frequently bent due to human
 247 body morphology and movements. Therefore, it is necessary to investigate the prototype
 248 performance characteristics under bending conditions. Figure 5 shows the output characteristic of
 249 the proposed BPF under bending condition.
 250

251
 252
 253
 254
 255
 256
 257
 258
 259
 260
 261
 262
 263
 264



265 **Figure 5.** Simulated effect of bending of wearable filter with different radii: 10, 30 and 40 mm.
 266

267 It is observed that by changing the radius of bending to 40 mm, the resonant frequency is shifted
 268 up 4.25 MHz/mm
 269
 270

271 5. Conclusions

272 A compact e-textile bandpass filter has been designed and successfully fabricated and tested. The
 273 proposed design is a fully embroidered conductive thread meander microstrip on textile substrate.
 274 A significant agreement is achieved for the EM layout simulations, equivalent circuit model and the
 275 experimental results. The measurement results exhibit a well-defined band-pass at center frequency
 276 of 7.58 GHz, with return loss of -29 dB and -11 dB for the insertion loss while, simulated return loss

277 response is -35 dB and insertion loss is - 0.5 dB. The proposed filter has advantages of miniature
278 size, flexible, durable and ease of washing and also suitable for applications in health management
279 based on signal monitoring and sports.

280
281
282

283 **Funding:** This research was funded by the Spanish Government MINECO under Project TEC2016-
284 79465-R.

285 **Conflicts of Interest:** The authors declare no conflicts of interest.

286

287 **References**

288

289 1. Lancaster, J. S. Development of new microstrip pseudo-interdigital. *IEEE Microwave Guided Wave Letter*,
290 261-263, 1995.

291 2. Eiyong Park, Daecheon Lim and Sungjoon Lim, Dual-Band Band-Pass Filter with Fixed Low Band and
292 Fluidically-Tunable High Band, *Sensors*, vol. 17, pp. 1884; doi:10.3390/s17081884, 2017.

293 3. M. Makimoto and S. Yamashita, Bandpass filters using parallel coupled strip line stepped impedance
294 resonators, *IEEE Trans., MTT-28*, 1980, 1413–1417.

295 4. Klemm, M. T. Textile UWB antennas for wireless body area. *IEEE Trans. Antennas Propag*, 3192–3197, 2006.

296 5. Elliot, P. e. E-textile microstrip patch antennas for GPS. *IEEE/ION Position Location and Navigation Symp*,
297 66-73, 2012.

298 6. Paradiso, R. L. A wearable health care system based on knitted integrated sensors. *IEEE Trans. Inf. Technol.*
299 *Biomed., Publ. IEEE*, 337–344, 2005.

300 7. B.Moradi, R. F.-G. E-Textile Embroidered Metamaterial Transmission Line for Signal Propagation Control.
301 *Material*, 2018.

302 8. Hong Jia-sheng, Lancaster M J. *Microstrip filters for RF/microwave applications*. New York: John
303 Wiley&Sons.

304 9. M Makimoto and S Yamashita, 1979. Compact Bandpass Filters Using Stepped Impedance Resonators,
305 *Proceedings of the IEEE*, Jan. 1979, vol. 67, p. 16-19.

306 10. D. Pozar, *Microwave Engineering*, New York: John Wiley&Sons.